# Eco-Friendly Sustainable Gamma Shielding Materials: GEANT4-Based Comparative Radiation Attenuation Study of Jute, Palm Fiber, and Beeswax

MD. EBRAHIM HASAN EMON, ROSHLAN RAHMAN DIPTO, ABDUS SATTAR MOLLAH*
Department of Nuclear Science & Engineering (NSE)
Military Institute of Science and Technology (MIST)
Mirpur Cantonment, Dhaka
BANGLADESH

**Corresponding author*

*Abstract:* - The requirement to switch out conventional shields made of hazardous or energy-intensive materials with ones made of biodegradable and environmentally friendly materials. Jute and palm fiber are cheap, readily available, and renewable resources, especially in developing countries. Natural fiber composites are ideal for applications where weight is a critical factor since they are typically thinner than traditional materials (such as portable shielding or aerospace). In this paper, the gamma radiation attenuation properties of locally available materials in Bangladesh, including untreated and treated jute fiber, untreated and treated oil palm pressed fiber (OPPFF), and beeswax, are discussed as potential alternatives to lead for radiation shielding. Using Geant4, a Monte Carlo simulation tool, the study models particle transport through matter. Gamma radioisotopes with photon energies ranging from 0.1 to 20 MeV were used to simulate the transport of 1,000,000 particles through the materials. The linear attenuation coefficient (μ), mass attenuation coefficient ($\mu_m$), and half-value layer (HVL), tenth-value layer (TVL), and the mean free path were calculated for each material, and the results were validated against the XCOM values. This study explores the possibilities of readily available, inexpensive, and biodegradable natural materials- beeswax, jute, and palm fiber- as eco-friendly substitutes for gamma radiation shielding. Because of their significant concentration of low-Z elements (carbon, hydrogen, and oxygen), the GEANT4 simulation results verify that jute, palm fiber, and beeswax have measurable gamma radiation attenuation capabilities, mostly through Compton scattering. In nuclear medicine clinics or PET/CT facilities, the sustainable composite materials- jute and palm fibers embedded in a beeswax matrix, perhaps with a tiny amount of non-toxic bismuth oxide ($Bi_2O_3$) filler- can be used to create movable secondary radiation shielding barriers.

*Key-Words:* - Jute fiber, Oil palm fiber, Bees-wax, Linear attenuation coefficient, Mass attenuation coefficient, GEANT4, Radiation.

Received: March 22, 2025. Revised: July 25, 2025. Accepted: August 26, 2025. Published: May 22, 2026.

## 1 Introduction

In industries including nuclear medicine, industrial radiography, and space exploration, there is an increasing need for radiation shielding materials that are safe for the environment, lightweight, and efficient. The idea of substituting conventional heavy shields like concrete and lead with natural materials, or biomaterials, is becoming more and more popular. The expected use of natural fibers, especially jute, as eco-friendly alternatives to composite applications remains untapped. Light, mechanically strong, renewable, and biodegradable natural fibers such as jute, palm fiber, banana, and bamboo are currently being studied as potential polymer composite reinforcements to address the growing environmental concerns. To address the growing environmental issues, the natural fiber reinforced polymer composites are gaining popularity due to their strength, corrosion resistance, low cost, and environmental sustainability. They find use in the automotive, aerospace, and biomedical industries [1]. It could provide gamma radiation protection. This ability to provide radiation shielding is particularly important in advanced engineering applications that eco-friendly reduce radiation exposure [2]. Jute, which is considered an important potential composite enhancing material, is due to its high cellulose content and its durability. It improves the tensile strength, toughness of the composite, and resistance to harsh environments. The study also assesses the effect of gamma radiation on enhancing the interfacial adhesion between the jute fibers and the polymer matrices; thus, the composite improves its performance [3]. Also, fiber-based composites are analyzed as safer, lighter, and greener alternatives for conventional radiation shielding materials such as lead, which reduce gamma radiation exposure in many instances [4]. Also, the study focuses on the collection of jute and oil palm fibres aimed at decreasing agricultural waste and improving sustainability. The study aims at increasing the collection of these fibres and the mechanical properties resulting from the application of surface treatments, which will also enhance their effectiveness in the composite [5] [6]. To identify useful and sustainable materials for radiation protection shielding Bangladesh's radiation facilities, researchers consider the potential of low-cost, locally available, and green materials [7] [8]. Low-cost and practical materials are also available as boluses in cancer treatments. The locally used beeswax has radiation attenuation properties equivalent to water and organic tissue. The use of BolusCM material in 3D printing of personalised bolus is also inexpensive, shows homogeneity, and is adequate for electron radiotherapy in skin cancer [9] [10].

The need for environmentally friendly and biodegradable materials to take the place of conventional shields that are hazardous or require a lot of energy. Agricultural byproducts like jute and palm fiber provide an inexpensive, easily accessible, and renewable resource, particularly in underdeveloped nations. There are studies on the mechanical and shielding characteristics of individual natural fiber composites (usually for neutron shielding), but there aren't many thorough, comparative simulation studies that concentrate on the gamma radiation attenuation performance of raw/pure jute, palm fiber, and beeswax using a standardized, sophisticated simulation framework like GEANT4. For gamma-shielding qualities at clinically and industrially relevant energy levels, a head-to-head comparison of all three materials is lacking, particularly beeswax, which has a high hydrogen content.

Natural fiber composites are perfect for situations where weight is a crucial consideration because they are usually less thick than conventional materials (e.g., aerospace, portable shielding). In this study, we investigate the gamma radiation attenuation properties of jute, palm fibers, and beeswax. The parameters related to gamma radiation attenuation involve the mass attenuation coefficient, the half value layer (HVL), the tenth value layer (TVL), and the mean free path, which have been calculated. The results of this study will help to use locally available jute, palm fiber, and beeswax, which are used as bolus materials in radiation therapy. The paper aims to,

1. To calculate the radiation attenuation properties using the Geant4 Monte Carlo code.
2. Evaluation of Jute and Palm fiber as gamma radiation shielding material, also to evaluate properties of bees wax for potential use as bolus materials during treatment of cancer patients.
3. To compare jute and palm fibers with locally available beeswax.

Examine earlier research that effectively used GEANT4 to characterize radiation shielding materials, confirming the use of simulation physics lists and geometry. Examine the body of research on the radiation-shielding capabilities of other natural fiber composites, such as wood composites and coconut fiber, with an emphasis on how well they work against gamma rays. This study is the first to directly compare three different sustainable biomaterials (jute, palm fiber, and beeswax) for gamma shielding using a single GEANT4 model. A thorough, high-resolution examination of particle contact and energy deposition is made possible by the use of GEANT4, which is not always practical or economical in an entirely experimental situation.

# 2 Theoretical Background

## 2.1 Photon Interaction Mechanisms and Cross-Section

The total interaction cross-section per atom for gamma-rays is given by the sum of the interaction cross-sections for photoelectric effect, pair production, and Compton scattering [11]:

$$\sigma (E) = \sigma_{pe} (E) + \sigma_{pp} (E) + \sigma_{c} (E)$$

Additionally, a macroscopic interaction cross-section may be defined by the multiplication of the microscopic interaction cross-section ($\sigma$) by the number density of atoms (N), which is called an attenuation coefficient and is denoted by the symbol ($\mu$).

$$\mu = \mu_{pe} + \mu_{pp} + \mu_{c}$$

Where ($\mu$) is the total attenuation coefficient for gamma-rays and ($\mu_{pe}$), ($\mu_{pp}$), ($\mu_{c}$) are the three interaction processes for gamma-rays. Units for ($\mu$) are $m^{-1}$ or $cm^{-1}$.

Also, it may be expressed as a mass-normalized attenuation coefficient; this is referred to as the mass attenuation coefficient.

$$\frac{\mu}{\rho}(E) = \left(\frac{\mu pe}{\rho}\right) + \left(\frac{\mu C}{\rho}\right) + \left(\frac{\mu pp}{\rho}\right)$$

### 2.1.1 Photoelectric Effect

The photoelectric effect has the strongest impact on interactions at lower photon energy levels, and it is significantly dependent upon both the atomic number (Z) of the material and the photon energy level (E). The approximate relationship of the photoelectric cross-section to these factors is given as follows:

$$\sigma_{pe} \propto Z^n$$

Where n is the function of E. This would explain why there is an increased attenuation observed in low-energy interactions (≤ 0.5 MeV), particularly with treated jute fibers that have higher effective atomic numbers than the untreated jute fibers due to the presence of Si, Fe and Ca, etc.

### 2.1.2 Compton Scattering

In the intermediate energy range (0.5–5 MeV), Compton scattering dominates. Its cross-section depends primarily on electron density rather than Z. An atom with atomic number ***Z***, has Z electrons. If the Compton cross-section for one free electron is ${}_e\sigma_C$ , then the total Compton cross-section for the entire atom is just the sum of the contributions from all its electrons.

$$\sigma_C \propto Z\ {}_e\sigma_C$$

Since jute, palm fiber, and beeswax are rich in low-Z elements (C, H, O), their attenuation behavior converges in this region, as observed in Table 2 and Table 3 (Appendix)

### 2.1.3 Pair Production

For photon energies exceeding 1.022 MeV, pair production becomes significant, with a cross-section approximately proportional to:

$$\sigma_{pp} \propto Z^2$$

In fact, all studied materials are composed mainly of low-Z elements, and pair production contributes modestly, resulting in similar attenuation coefficients at high energies (>5 MeV).

## 2.2 Calculation of Linear and Mass Attenuation Coefficient

### 2.2.1 Linear Attenuation Coefficient (μ):

The attenuation coefficient is an important parameter for the study of the interaction of radiation with matter and indicates the fraction of energy scattered or absorbed. The probability of a photon interaction with a given material, per unit path length, is called the 'Linear Attenuation Coefficient'. This coefficient is of great importance in radiation shielding materials.

When gamma-rays traverse a small thickness of matter, dx at any point in a medium, the extent of interaction of the photons is proportional to the radiation intensity at the point and to the thickness traversed. Consequently, in traversing the distance dx, the intensity of the gamma-ray photons, which have not undergone interaction, will be decreased by as follows.

$dI = -\mu I dx$ or $\frac{dI}{I} = -\mu dx$

Integrating the above equation, we get,

$I = I_0 e^{-\mu x}$ ... ... (1)

This process follows Beer-Lambert's Law. In this relation, $I_0$ refers to the intensity of initial radiation, I, the intensity after radiation has penetrated an x thickness of an absorbing medium, and μ, the proportionality constant (generally called the attenuation coefficient) expressed in $m^{-1}$ or $cm^{-1}$ units.

### 2.2.2 Mass Attenuation Coefficient (μ/ρ):

The mass attenuation coefficient is defined as the linear attenuation coefficient divided by the material density:

$\mu_m = \frac{\mu}{\rho}$ … … (2)

Where ρ is the physical density of the shielding material.

This quantity represents the attenuation capability per unit mass and allows direct comparison of different materials regardless of their physical density.

$I = I_0 e^{-(\mu/\rho)(\rho x)}$

The total mass attenuation coefficient ( $(\mu/\rho)_{compound\ or\ mixture}$ for any chemical compound or mixture of elements is given by the mixture rule [12]:

$(\mu/\rho)_{compound\ or\ mixture} = \sum_i \left(\frac{\mu}{\rho}\right)_i w_i$

where $w_i$ and $(\mu/\rho)_i$ are the weight fraction and mass attenuation coefficient of the i$^{th}$ constituent element, respectively. For a chemical compound, the fraction by weight $(w_i)$ is given by,

$w_i = \frac{niAi}{\sum_j njAj}$

where $A_i$ is the atomic weight of the i$^{th}$ element, and $n_i$ is the number of formula units, and $\Sigma_i w_i = 1$.

## 2.3 Calculation of HVL and TVL

The Half Value Layer (HVL) is the thickness of a shield or shielding material where, following attenuation, the radiation intensity is decreased by a factor of two. This term is addressed through the equation as follows [12]:

HVL = ln2/μ = 0.693/μ ... … (3)

The Tenth Value Layer (TVL) is denoted as the thickness at which radiation is reduced to 10% of its initial level following attenuation is known as the Tenth Value Layer (TVL). It is determined by the following equation:

$$TVL = \ln 10/\mu = 2.3026/\mu \quad \ldots \quad \ldots \quad (4)$$

### 2.4 Calculation of Mean Free Path

The relaxation length (λ), also called the photon mean free path, is the average distance between two successive interactions, which is determined by the following equation [12]:

$$\lambda = \frac{\int_0^\infty x e^{(-\mu x)} dx}{\int_0^\infty e^{(-\mu x)} dx} = 1/\mu \quad \ldots \quad \ldots \quad (5)$$

Where the mean free path in centimetres is represented by the Greek symbol λ (lambda). The mean free path between consecutive collisions is rarely a straight line because electrons scatter photons as they travel.

### 2.5 Energy-Dependent Origin of Mass Attenuation Coefficients

The mass attenuation coefficients reflect the chance that a photon will interact with each unit of mass as it passes through matter and are thus fundamentally dependent on the energy of the photons involved in the interactions. At low photon energies, the relatively large cross-sectional area associated with photoelectric absorption results in large attenuation coefficients; at higher photon energies, the reduced interaction probability causes the attenuation coefficients to be less than those measured at lower photon energies. This trend is illustrated by the data in Figure 2, where the attenuation coefficients are monotonically decreasing (with increasing photon energy) for all three material systems studied.

## 3 Methodology

### 3.1 Materials and Models

The mass attenuation coefficient has been determined for seven different shielding materials-

- Untreated Jute Fiber
- Treated Jute Fiber
- Untreated Oil Palm Pressed Fruit Fiber (OPPFF)
- Treated Oil Palm Pressed Fiber (OPPFF)
- Bee Wax (BM1)
- Bee Wax (BM2)
- Bee Wax (BM3)

We used equations (1) and (2) to figure out the mass attenuation coefficient for each of the seven shielding materials in the gamma energy ranges of 0.1 to 20 MeV, which were used to find the mass attenuation coefficients of these samples throughout the specified energy range and also used the same gamma radiation sources to figure out the HVL, the TVL, and the Mean Free Path. Both elemental composition (% weight fraction) and density (g/cm3) of Jute, Palm Fibre, Bees wax from literature, the developed bees wax (Bees wax KYAU), and commercial bolus material are noted in Table 1 (Appendix). The present study represents the modelling of radiation shielding materials 2using the Geant4 simulation toolkit.

#### 3.1.1 GEANT4 Setup for Simulation

The geometry, materials, primary particle source, and relevant physics list must be specified in order to set up a Geant4 simulation for gamma-ray radiation. Geant4's main function is to track particles and use Monte Carlo techniques to model how they interact with matter. A brief description of GEANT4 simulation setup is given below:

• Source: Specify the energy levels of the gamma source (such as a point source).

• Geometry: Construct the simulation environment and position a slab of material with different thicknesses between a detector and the source.

• Physics List: To accurately describe gamma-ray interactions, choose a suitable GEANT4 physics list (such as G4EmStandardPhysics_option3 or a comparable high-precision electromagnetic physics list).

• Detector: To evaluate the reduced intensity, define a sensitive detector.

• Execution: Run the simulation for a number of main particles that is statistically significant.

Focusing on materials that are locally developed and readily available. In this model, a cylindrical radiation source has been utilized to generate the required radiation. A generic 2D setup is shown in Figure 1a.

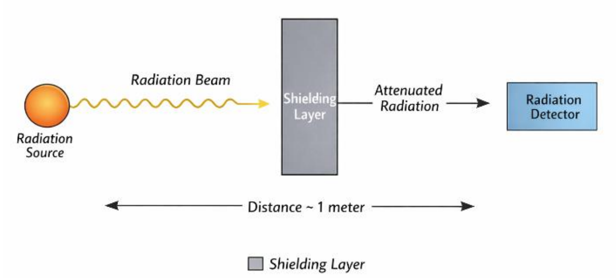


Fig. 1a: GEANT4 radiation shielding simulation schematic diagram with a single shield layer.

*Source: created by the authors.*

The typical geometry produced through the GEANT4 simulation is illustrated in Figure 1b. In this study, a radiation source and a NaI detector were modelled in Geant4 to test shielding effectiveness. A slab of shielding material was placed between the source and detector. The detector first measured the radiation ($I_0$) absorbed without shielding, and then the mass attenuation coefficient was determined by repeating the test with the material slab. The absorbed dose (I) was calculated in the detector. The gamma-ray production and attenuation process was simulated, and the mass attenuation coefficient was computed using equation (1). The gamma photons emitted by the source have been detected using a detector made of a cube-shaped NaI. Also, a slab-shaped shield has been used in this research.

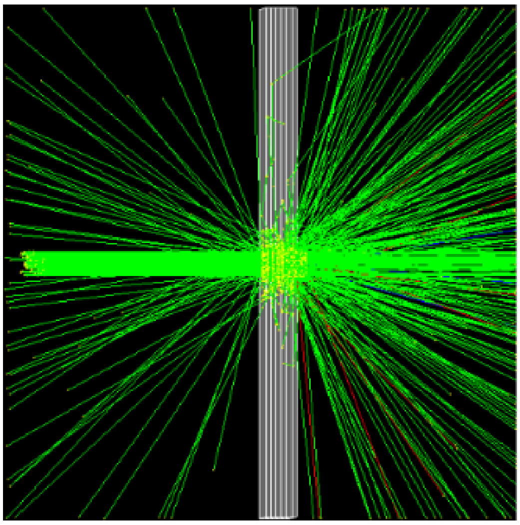

Fig. 1b: The process of gamma-ray production and interaction is modelled within the GEANT4 software.
*Source: created by the authors.*

### 3.1.2 Electromagnetic Physics Modeling in GEANT4

Photon interactions were simulated using the GEANT4 standard electromagnetic physics list, which includes evaluated cross sections for photoelectric absorption, Compton scattering, and pair production, with an accuracy of approximately 1–3% relative to experimental data and NIST references [13]. The simulation assumes homogeneous materials, monoenergetic photon sources, and neglects secondary neutron production, which is negligible for the energy range and materials considered. To minimize statistical uncertainty, $10^6$ primary photons were simulated per energy point. The selected physics list provides reliable coverage over the MeV–GeV energy range relevant to this study, while higher-energy processes such as bremsstrahlung and pair production have been extensively validated in high-energy detector applications.

### 3.1.3 Result and Discussion

The simulated μ/ρ values for the materials above using Geant4 are listed in Table 2 and Table 3 (Appendix). Additionally, this table lists the theoretical values obtained by the XCOM program to validate our results. It is evident that the simulated results from Geant4 are close to those obtained by XCOM, and this indicates the accurate values for the μ/ρ values for the developed jute and palm fibers, along with bees wax (Bees wax KYAU) samples. The deviations between the simulated and XCOM obtained values are very small for all samples. The Root mean square difference between Geant4 and XCOM values for untreated and treated jute was found to be 0.000318 and 0.000549, respectively. The RMS difference for untreated and treated oil palm was found to be 0.000376 and 0.000396. Finally, for BM1, BM2, and BM3, the simulation obtained value and XCOM value's RMS difference was 0.000494, 0.0004941, and 0.00046, respectively.

## 3.2 Total mass attenuation coefficient ($\mu_m$)

According to Figure 2 and as presented in Table 2 and Table 3 (Appendix), as gamma-ray energy increases, the mass attenuation coefficients of fiber-based shielding materials decrease. The photoelectric effect predominates at low energies (<0.1 MeV), with treated jute demonstrating the highest attenuation, which is almost double that of untreated jute. Untreated and treated palm fiber show better attenuation power at the low energy range than untreated jute fiber. The beeswax samples show the lowest mass attenuation coefficient due to low density. Among the three beeswax sample materials, the BM3 sample shows better mass attenuation power than the other two samples. Moreover, the Compton effect makes gamma-ray shielding difficult because the scattered photon doesn't vanish after the interaction. Instead, it keeps traveling and can cause further interactions, and this Compton effect is dominant in the intermediate-energy range for photon interactions, roughly between 0.1 MeV and a few MeV. For this reason, the mass attenuation decreases drastically. Although treatment has little to no adverse effects, oil palm pressed fibre (OPPFF) likewise exhibits greater attenuation than untreated jute. Attenuation values converge, and Compton scattering takes over as energy increases (0.1–1 MeV). All materials exhibit comparable shielding effectiveness at high energies, with treatment effects becoming negligible and coefficients (0.016–0.006 $cm^2/g$) above 1 MeV. As in the high energy range of gamma photons, the pair production dominates, and the probability increases with the square of the atomic number ($Z^2$). It occurs when a high-energy photon (greater than 1.02 MeV) converts into an electron–positron pair in the electromagnetic field of a nucleus, which effectively reduces the original photon's energy [11].

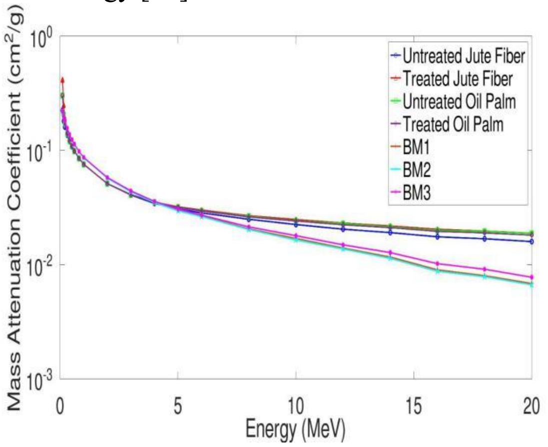


Fig. 2: Mass attenuation coefficients for different materials ($cm^2/g$).
*Source: created by the authors.*

### 3.2.1 The Half Value Layer (HVL)

Half Value Layer (HVL) is described as the thickness of the material that is required to decrease photon intensity by half of its original value. A lower HVL value represents a better ability of the material to shield as much as possible. Based on the values in Table 3 (Appendix) and as plotted in Figure 3, the natural fibers such as jute and oil palm have HVL values at low energies (0.1–0.5 MeV) that have a low range of at least 1 to 5 cm, meaning that these materials can attenuate low-energy photons. Photons attenuated by jute show a pattern of jute value that is lower than HVL, the fraction of energy that is low by jute is likely better than untreated attenuation photon. This pattern is similar to that observed in oil palm fibres, although there is a smaller difference between untreated and treated. The difference is the range of natural fibres, such as the bee-composite wax BM1, BM2, and BM3, that show HVL over values are significant at all energies, and most at low energies. The best of these bee-composite wax materials is BM3, which bears the least HVL indicative, and thus is most effective. Among all materials, HVL values for photon energies are at a lower level, and hence the HVL values are at a lower level. This means that the photoelectric characteristic effect is dominant, which absorbs the photon level on a lower energy level at a high density, high-Z materials. In the 0.5-5 MeV range, the presence of Compton scattering creates a higher HVL as a result of the photons continuing along their paths after losing some energy, thus requiring a thicker slab of radiation for protection. For the higher energy level, >5 MeV, the HVL becomes much larger, pair production dominates the interaction processes, with over 20 cm for the composite and over 15 cm for the fibers involving the annihilation photons of 0.511 MeV that must also be shielded. From the obtained results, BM3 is the most effective of the studied composites, and the treatment helps to increase the attenuation of the natural fibers, and the considerable energy of the photon is what determines the thickness of the required material that is needed for radiation shielding.

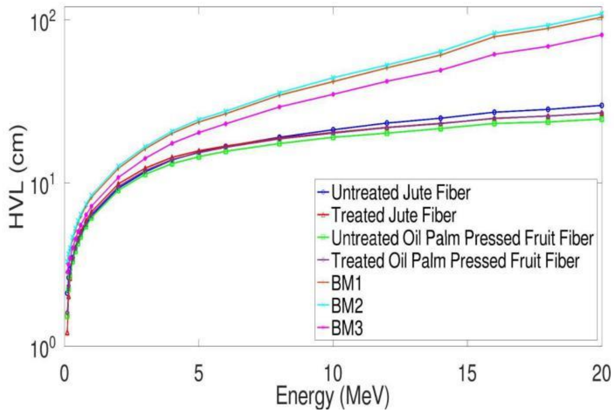


Fig. 3: HVL values for the investigated sample materials (cm).
*Source: created by the authors.*

### 3.2.2 The Tenth Value Layer (TVL)

The Tenth Value Layer (TVL) is an indication of how BM composite and natural fibres perform as shielding materials over various photon energies (Figure 4). The TVL is the thickness of material needed so that when a slab of material is placed, it will reduce the photon intensity to one-tenth of the original value. Hence, the lower the TVL, the better the shielding materials. The natural fibres, both jute and oil palm, withstand lower TVL values at lower energies (0.1–0.5 MeV) in the range of approximately 4–15 cm Table 6 and Table 7 (Appendix). Treated jute consistently had lower values than untreated jute; this is evidence that treatment facilitates photon attenuation. Oil palm fibres exhibited a similar pattern, but the treatment of the fibre appears to be less pronounced. All fibres tested showed increased values of TVL at 20 MeV in the range of 80–90 cm, meaning that there is less shielding effectiveness at higher energies. There is a steady growth of 80–90 cm at 20 MeV with oil palm, reflecting less shielding effectiveness. While there were some similar patterns, the beeswax composites in general had greater TVL values than these fibres, particularly with the higher energies. BM3 is the most effective of the three composites, as it consistently had lower values compared to BM1 and BM2. Here, BM3 had a TVL of about 9.5 cm at 0.1 MeV, which was lower than that of BM1 and BM2, and at 20 MeV, it had a TVL of about 268 cm, which was also lower than that of BM1 and BM2. This advantage remained at the higher energies due to the continued performance advantage of BM3, even as TVL rose significantly. The rise in the energy of the photons had an impact on all materials. TVL grew marginally as the energy increased. At low energies (≤0.5 MeV), TVLs were low because of the predominance of the photoelectric effect, which permits effective absorption of the photon. The main interaction process in the intermediate energy range (0.5–5 MeV) was Compton scattering, in which photons are not completely absorbed, scattering instead and increasing the thickness of needed shielding. At higher energies (>5 MeV), the pair production of the dominant interaction and the TVL values increased markedly. The need for shielding in this range is increased because the accompanying annihilation photons of 0.511 MeV created by the secondary photons also need to be absorbed. The overall conclusion is that treated jute fiber is better than all the other composites, and treatment increases the fiber's effectiveness, while the energy of the photon significantly lowers the thickness of the required shielding material.

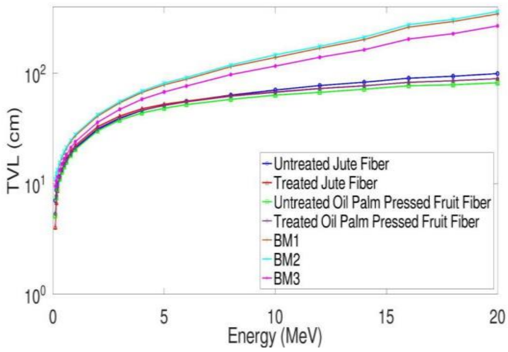


Fig. 4: TVL values for the investigated sample materials.
*Source: created by the authors.*

### 3.2.3 Mean Free Path

The acquired MFP data indicate how different materials behave while attenuating different energy photons. This is summarized in detail in Figure 5 alongside Table 8 and Table 9 (Appendix). The MFP is the distance a photon travels in a material before it interacts. When the MFP value is lower, it is indicative that more material is able to shield the photons. In the (>5 MeV) region, it is apparent and consistent that treated jute MFP values are lower than those of untreated, further substantiating the conclusion that treatment helps photons get attenuated by jute. This is also the case in jute with oil palm fibres, with a lesser improvement than jute in MFP values due to treatment. In the low region, the MFP values of the materials are relatively low, with values equal to 1.7–6.5 cm for fibres. This is a clear demonstration of the materials (especially the fibres) having the ability to attenuate the photons by virtue of the photoelectric effect. On the other hand, the MFP values keep increasing with photon energy, and at 20 MeV, it is over 35 cm, which signals less photon interaction in this range. Compared to natural fibers, the BM composites have generally MFP values that are higher, especially at higher energies. However, BM3 MFP is the lowest out of the three composites, making it the most efficient composite at photon attenuation. For instance, at 0.1 MeV, the MFP of BM3 is about 4.1 cm, which is lower than that of BM1 and BM2, and this low MFP is retained throughout energies. The difficulty of shielding against high-energy photons is highlighted by the fact that all BM composites exhibit a sharp increase in MFP as photon energy increases, exceeding 100 cm beyond 16 MeV. As the photon energy increases, the MFP value of every material is affected noticeably. At low energies, the dominance of the photoelectric effect ensures shorter mean free paths and more efficient attenuation. In the intermediate energy range (0.5–5 MeV), Compton scattering is the dominant interaction. As a result, the mean free path gradually increases, since photons continue to travel even after losing part of their energy. At high energies (>5 MeV), the pair production becomes the dominant process, which causes the MFP value to increase significantly. The annihilation photons of energy 0.511 MeV that result from pair production add to the radiation load and raise the mean free path, even though pair production lowers the photon's energy by creating an electron–positron pair. Overall, the findings indicate that BM3 is the most efficient composite, while natural fibers, particularly treated jute, provide enhanced efficiency in photon absorption at low energies. However, for all materials to maintain effective shielding, much greater thickness must be present as the photon energy increases.

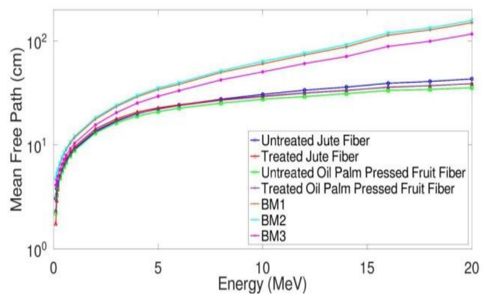


Fig. 5: The Mean free path (in cm) for the investigated sample materials.
*Source: created by the authors.*

### 3.3 Quantitative Interpretation of Shielding Performance

It has been found that the shielding properties of these composite materials are influenced by the two variables of the material's density and its element content, with the linear attenuation coefficient being the result of both factors [9]. Therefore, higher densities and the presence of elements with a greater atomic number (Z), results in a higher probability of interaction of the incident photons, with the photoelectric effect having a dominant influence on this type of interaction at lower photon energies; consequently, this will lead to a greater degree of attenuation of the photons, and therefore smaller values of the half-value layer (HVL).The superior shielding properties of chemically treated jute fibers can be directly related to their increased effective atomic number and density when compared to untreated jute. For example, at a photon energy of 0.1 MeV, it was determined that the mass attenuation coefficient of treated jute was 0.4148 $cm^2 \cdot g^{-1}$, while the mass attenuation coefficient of untreated jute was 0.2239 $cm^2 \cdot g^{-1}$. Consequently, the HVL for treated jute was approximately 45% less than for untreated jute Table 4 (Appendix). The large improvement in HVL values for treated jute is a direct result of the large degree of photoelectric absorption occurring due to the increased concentration of $Z > 10$ elements (such as silicon and iron), which were added to the jute during the chemical treatment process.

Similar trends are seen among the beeswax samples as well. The BM3 sample shows the lowest HVL, TVL, and MFP across the entire range of energies that were studied. The reason for this trend can be directly attributed to the higher density of BM3 (1.11 $g/cm^3$) and its high hydrogen content, both of which lead to higher electron densities and therefore increase the likelihood of Compton scattering occurring when BM3 is exposed to photons [9]. As an example, at 0.1MeV, the HVL value of BM3 is approximately 2.85 cm, while the HVL for BM1 was found to be 3.21 cm, indicating that BM3 has a much stronger ability to attenuate photons Table 5 (Appendix).

Photons will lose energy when passing through a material by losing energy that is absorbed in an interaction with the atoms of the material (photoelectric effect) or by transferring some of their energy to an electron (Compton scatter). As the energy of the photons increases, the frequency of photoelectric interactions decreases while the frequency of Compton scatters increases; thus, the total interaction rate of the photons with the atoms of the material will be higher than it would have been at lower energies, and therefore the half-value layer (HVL) will be larger than it would have been at lower energies [14] [15].

However, if the material is rich in oxygen, it will have better low-energy attenuation. If the material is rich in carbon or polymer, it will exhibit attenuation characteristics similar to those exhibited by biological tissues, making it suitable for use in tissue equivalent shielding applications [9] [10].

These findings demonstrate a clear relationship, both quantitatively and physically, between the elemental composition of a material, the density of the material, the methods of interaction between the photons and the material, and the observed degree of shielding provided by the material. These relationships provide a strong foundation upon which to optimize the development of new eco-friendly radiation shielding materials.

## 4 Conclusion

According to the research, locally accessible natural fibres like jute and oil palm fibre, and beeswax can be good gamma shielding materials. When jute and palm fibres are properly treated, they may be good substitutes for conventional radiation shielding materials like lead, especially for the low to medium-energy gamma radiation. Among them, the treated jute fiber is the most preferable for shielding. In addition, the findings suggest that locally available beeswax has the potential to serve as an effective bolus material. It is inexpensive, easy to shape to the patient's body, and has properties similar to human tissue. This makes beeswax a practical choice for use in cancer treatment. Among the tested samples, BM3 proved the best shielding ability. But among the seven samples, treated jute is the best for attenuating gamma, and it can be suggested to use it for low to medium range gamma energy. Overall, these materials are perfect for use in radiation therapy rooms, waste storage facilities, and nuclear research because they are affordable, lightweight, and environmentally friendly. In radiation protection applications, this paper promotes the use of sustainable and environmentally friendly fiber-based materials as viable alternatives to traditional radiation shielding, offering both environmental and economic benefits.

The sustainable composite materials- jute and palm fibers embedded in a beeswax matrix, possibly combined with a small quantity of non-toxic bismuth oxide ($Bi_2O_3$) filler- can be used to produce movable secondary radiation shielding barriers in nuclear medicine clinics or PET/CT facilities. By deploying distributed, flexible, and sustainable shields to control the radiation dose in non-critical areas, this application changes the perspective from using enormous shields to block all radiation. By directly exploiting the beneficial characteristics measured by the GEANT4 comparison study, the final product is a non-toxic, lightweight, and mobile barrier that efficiently controls ambient dose rates and secondary scatter in patient-centric settings.

*Acknowledgments*
The authors show their gratitude to the Department of Nuclear Science and Engineering at the Military Institute of Science and Technology for providing all the essential facilities.

*References*:

[1] Motaleb, K. A., Milašius, R., and Ahad, A. (2020). Influence of gamma radiation on the mechanical properties of Jute Fabric-Reinforced polymer composites. Fibers, 8(9), 58. https://doi.org/10.3390/fib8090058

[2] Amir, S. M., Sultan, M. T., Jawaid, M., Safri, S. N., Shah, A. U., Yusof, M. R., Naveen, J., Mohd, S., Salleh, K. A., and Saba, N. (2019). Effects of layering sequence and gamma radiation on mechanical properties and morphology of Kevlar/oil palm EFB/epoxy hybrid composites. Journal of Materials Research and Technology, 8(6), 5362–5373. https://doi.org/10.1016/j.jmrt.2019.09.003

[3] Rahman, H., Yeasmin, F., Islam, T., Hasan, M., Uddin, M. B., & Khan, R. A. (2022). Fabrication and investigation of the physico-mechanical properties of Jute-PALF reinforced LLDPE hybrid composites: Effect of gamma irradiation. Heliyon, 8(4), e09287. https://doi.org/10.1016/j.heliyon.2022.e09287

[4] Okafor, C. E., Okonkwo, U. C., and Okokpujie, I. P. (2021). Trends in reinforced composite design for ionizing radiation shielding applications: a review. Journal of Materials Science, 56(20), 11631–11655. https://doi.org/10.1007/s10853-021-06037-3

[5] Daramola, O. O., Balogun, O. A., Adediran, A. A., Saka, S. O., Oladele, I. O., & Akinlabi, E. T. (2021b). Tensile, flexural, and morphological properties of Jute/Oil palm pressed fruit fibers reinforced high-density polyethylene hybrid composites. Fibers, 9(11), 71. https://doi.org/10.3390/fib9110071

[6] Ibrahim, Z., Ahmad, M., Aziz, A. A., Ramli, R., Wahab, N. A., Alias, A. H., Osman, S., and Sheng, E. L. (2020b). Oil palm empty fruit bunches (EFB): Influence of alkali and acid treatment on the mechanical properties of medium density fibreboard (MDF). Journal of Advanced Research in Fluid Mechanics and Thermal Sciences, 79(1), 44–53. https://doi.org/10.37934/arfmts.79.1.4453

[7] Ramesh Kumar, R. (2025). Radiation shielding efficiency of eco-friendly composite materials against gamma and neutron radiation, International Journal of Applied and Behavioural Sciences (IJABS), Vol.02, Issue 02, 100-105. DOI: 10.70388/ijabs250141

[8] Shinoj, S., Visvanathan, R., & Panigrahi, S. (2010). Towards industrial utilization of oil palm fibre: Physical and dielectric characterization of linear low density polyethylene composites and comparison with other fibre sources. Biosystems Engineering, 106(4), 378–388. https://doi.org/10.1016/j.biosystemseng.2010.04.008

[9] Islam, S., Mahmoud, K., Sayyed, M., Alim, B., Rahman, M., and Mollah, A. S. (2019). Study on the radiation attenuation properties of locally available beeswax as a tissue equivalent bolus material in radiotherapy. Radiation Physics and Chemistry, 172, 108559. https://doi.org/10.1016/j.radphyschem.2019.108559

[10] Diaz-Merchan, J., Martinez-Ovalle, S., and Vega-Carrillo, H. (2023). Development of a 3D printing process of bolus using BolusCM material for radiotherapy with electrons. Applied Radiation and Isotopes, 199, 110899. https://doi.org/10.1016/j.apradiso.2023.110899

[11] Lamarsh, J. R., and Melkonian, E. (1977). Introduction to nuclear engineering. Physics Today, 30(6), 53, https://doi.org/10.1063/1.3037597

[12] Toyen, D., Wimolmala, E., Hemvichian, K., Lertsarawut, P., & Saenboonruang, K. (2024). Highly efficient and eco-friendly thermal-neutron-shielding materials based on recycled high-density polyethylene and gadolinium oxide composites. Polymers, 16(8),1139. https://doi.org/10.3390/polym16081139

[13] Allison, J., Amako, K., Apostolakis, J., Arce, P., Asai, M., Aso, T., Bagli, E., Bagulya, A., Banerjee, S., Barrand, G., Beck, B., Bogdanov, A., Brandt, D., Brown, J., Burkhardt, H., Canal, P., Cano-Ott, D., Chauvie, S., Cho, K., . . . Yoshida, H. (2016). Recent developments in Geant4. Nuclear Instruments and Methods in Physics Research Section A Accelerators Spectrometers Detectors and Associated Equipment, 835, 186–225. https://doi.org/10.1016/j.nima.2016.06.125

[14] Akkurt, I., and El-Khayatt, A. (2012). The effect of barite proportion on neutron and gamma-ray shielding. Annals of Nuclear Energy, 51, 5–9. https://doi.org/10.1016/j.anucene.2012.08.026

[15] M. Mostafa, Roshlan Rahman Dipto, A. S. Mollah and J. Kabir, Advanced Multilayer Composite Shielding for Spent Nuclear Fuel Casks: Geant4 Simulation and Validation with EpiXS, International Journal of Chemical Engineering and Materials, Vol. 4, 111-119, 2025 (November), DOI: 10.37394/232031.2025.4.9.

### Contribution of Individual Authors to the Creation of a Scientific Article (Ghostwriting Policy)

**Md. Ebrahim Hasan Emon -** Resources, Methodology, Data Curation, Original Draft Writing.
**Roshlan Rahman Dipto -** Formal Analysis, Data Curation, Resources, Methodology.
**Abdus Sattar Mollah -** Supervision, Conceptualization, Editing, Methodology, Resources.

### Sources of Funding for Research Presented in a Scientific Article or Scientific Article Itself

No funding was received for conducting this study.

### Conflict of Interest

The authors have no conflicts of interest to declare that are relevant to the content of this article.

Table 1 - Atomic Composition percentage of Jute, Oil Palm fibers, and Bee-wax materials

| Element | Untreated Jute Fiber ρ = 1.46 $gm/cm^3$ | Treated Jute Fiber ρ = 1.373 $gm/cm^3$ | Untreated Oil Palm Pressed Fruit Fiber (OPPFF) ρ = 1.503 $gm/cm^3$ | Treated Oil Palm Pressed Fruit Fiber (OPPFF) ρ = 1.425 $gm/cm^3$ | BM1 ρ = 0.98 $gm/cm^3$ | BM2 ρ = 0.96 $gm/cm^3$ | BM3 ρ = 1.11 $gm/cm^3$ |
|---|---|---|---|---|---|---|---|
| Ca | 5.2 | 4.5 | 5.5 | 5.0 | - | - | - |
| C | 14.4 | 8.5 | 10.0 | 11.0 | 81.16 | 79.24 | 84.17 |
| O | 32.0 | 14.0 | 18.0 | 16.0 | 5.18 | 0.21 | 0.09 |
| Mg | 3.5 | 4.0 | 3.0 | 3.0 | - | - | - |
| Fe | 3.9 | 11.0 | 11.5 | 11.0 | - | - | - |
| Si | 30.6 | 55.0 | 51.0 | 53.0 | - | - | - |
| Na | 1.3 | - | - | - | - | - | - |
| K | 2.9 | - | - | - | - | - | - |
| S | 6.2 | - | - | - | - | 0.21 | 0.09 |
| Au | - | 3.0 | 1.0 | 1.0 | - | - | - |
| H | - | - | - | - | 13.58 | 11.76 | 14.02 |
| N | - | - | - | - | 0.08 | 1.12 | 0.01 |

*Source: [6][[9]. Summarized by the authors.*

Table 2 - Mass attenuation coefficient for Jute and Oil Palm fibers

| Energy (MeV) | Mass attenuation coefficient ($cm^2/g$) | | | | | | | |
|---|---|---|---|---|---|---|---|---|
| | Untreated Jute Fiber | | Treated Jute Fiber | | Untreated Oil Palm Pressed Fruit Fiber | | Treated Oil Palm Pressed Fruit Fiber | |
| | XCOM | Geant4 | XCOM | Geant4 | XCOM | Geant4 | XCOM | Geant4 |
| 0.1 | 0.1825 | 0.2239 | 0.347 | 0.4148 | 0.2503 | 0.30078 | 0.2494 | 0.30154 |
| 0.15 | 0.1441 | 0.1799 | 0.1998 | 0.2491 | 0.1665 | 0.20604 | 0.1662 | 0.20675 |
| 0.2 | 0.1269 | 0.1601 | 0.1524 | 0.1928 | 0.1369 | 0.17176 | 0.1368 | 0.17241 |
| 0.3 | 0.1077 | 0.1359 | 0.1160 | 0.1468 | 0.1108 | 0.13931 | 0.1108 | 0.13985 |
| 0.4 | 0.09579 | 0.1196 | 0.09941 | 0.1245 | 0.09702 | 0.12078 | 0.09702 | 0.12122 |
| 0.5 | 0.08720 | 0.1075 | 0.08900 | 0.1100 | 0.08772 | 0.10808 | 0.08772 | 0.10832 |
| 0.6 | 0.08051 | 0.0981 | 0.08148 | 0.09967 | 0.08072 | 0.09828 | 0.08072 | 0.09850 |
| 0.8 | 0.07061 | 0.0851 | 0.07084 | 0.08566 | 0.07054 | 0.08486 | 0.07055 | 0.08515 |
| 1 | 0.06343 | 0.0754 | 0.06339 | 0.07567 | 0.06327 | 0.07518 | 0.06327 | 0.07537 |
| 2 | 0.04457 | 0.0511 | 0.04453 | 0.05111 | 0.04450 | 0.05108 | 0.04450 | 0.05113 |
| 3 | 0.03636 | 0.0406 | 0.03668 | 0.04096 | 0.03654 | 0.04078 | 0.03655 | 0.04085 |
| 4 | 0.03177 | 0.0343 | 0.03242 | 0.03516 | 0.03219 | 0.03509 | 0.03219 | 0.03493 |
| 5 | 0.02887 | 0.03078 | 0.02980 | 0.03204 | 0.02949 | 0.03180 | 0.02948 | 0.03172 |
| 6 | 0.02692 | 0.02831 | 0.02809 | 0.02997 | 0.02770 | 0.02948 | 0.02770 | 0.02939 |
| 8 | 0.02451 | 0.0249 | 0.02609 | 0.02677 | 0.02558 | 0.02642 | 0.02557 | 0.02611 |
| 10 | 0.02316 | 0.0224 | 0.02507 | 0.02476 | 0.02446 | 0.02419 | 0.02445 | 0.02406 |
| 12 | 0.02234 | 0.02039 | 0.02453 | 0.02305 | 0.02383 | 0.02283 | 0.02381 | 0.02229 |

| | | | | | | | | |
|---|---|---|---|---|---|---|---|---|
| 14 | 0.02182 | 0.01904 | 0.02425 | 0.02176 | 0.02348 | 0.02138 | 0.02346 | 0.02106 |
| 16 | 0.02151 | 0.0175 | 0.02413 | 0.02034 | 0.02330 | 0.01991 | 0.02328 | 0.01951 |
| 18 | 0.02131 | 0.01681 | 0.02412 | 0.01961 | 0.02323 | 0.01950 | 0.02321 | 0.01893 |
| 20 | 0.02120 | 0.0159 | 0.02417 | 0.01880 | 0.02323 | 0.01872 | 0.02321 | 0.01809 |

*Source: created by the authors.*

Table 3 - Mass attenuation coefficient for the Bee-wax sample material

| Energy (MeV) | Mass attenuation coefficient ($cm^2/g$) | | | | | |
|---|---|---|---|---|---|---|
| | BM1 | | BM2 | | BM3 | |
| | XCOM | Geant4 | XCOM | Geant4 | XCOM | Geant4 |
| 0.1 | 0.1710 | 0.2202 | 0.1697 | 0.2190 | 0.1718 | 0.2189 |
| 0.15 | 0.1525 | 0.1976 | 0.1513 | 0.1965 | 0.1533 | 0.1968 |
| 0.2 | 0.1393 | 0.1813 | 0.1382 | 0.1802 | 0.1401 | 0.1808 |
| 0.3 | 0.1209 | 0.1560 | 0.1199 | 0.1551 | 0.1216 | 0.1558 |
| 0.4 | 0.1082 | 0.1375 | 0.1074 | 0.1367 | 0.1088 | 0.1376 |
| 0.5 | 0.0988 | 0.1237 | 0.09803 | 0.1229 | 0.09937 | 0.1238 |
| 0.6 | 0.09136 | 0.1131 | 0.09065 | 0.1122 | 0.09189 | 0.1133 |
| 0.8 | 0.08023 | 0.0977 | 0.07961 | 0.0971 | 0.0807 | 0.0979 |
| 1 | 0.07139 | 0.0865 | 0.07157 | 0.0858 | 0.07255 | 0.0866 |
| 2 | 0.05031 | 0.0576 | 0.04992 | 0.05699 | 0.05059 | 0.0578 |
| 3 | 0.04021 | 0.0436 | 0.03989 | 0.0433 | 0.04042 | 0.04412 |
| 4 | 0.03425 | 0.0351 | 0.03399 | 0.03481 | 0.03441 | 0.03569 |
| 5 | 0.0303 | 0.02991 | 0.03007 | 0.0295 | 0.03042 | 0.03068 |
| 6 | 0.02749 | 0.02665 | 0.02728 | 0.02625 | 0.02759 | 0.0271 |
| 8 | 0.02376 | 0.02051 | 0.02359 | 0.02025 | 0.02382 | 0.02136 |
| 10 | 0.02142 | 0.01693 | 0.02126 | 0.01638 | 0.02145 | 0.01789 |
| 12 | 0.01982 | 0.01395 | 0.01968 | 0.01369 | 0.01983 | 0.01488 |
| 14 | 0.01867 | 0.01165 | 0.01854 | 0.01132 | 0.01866 | 0.01273 |
| 16 | 0.01781 | 0.009 | 0.01769 | 0.00873 | 0.01779 | 0.01018 |

| | | | | | | |
|---|---|---|---|---|---|---|
| 18 | 0.01716 | 0.008 | 0.01703 | 0.00782 | 0.01711 | 0.0091 |
| 20 | 0.01664 | 0.00683 | 0.01652 | 0.00664 | 0.01659 | 0.00774 |

*Source: created by the authors.*

Table 4 - HVL Values (cm) for Jute and Oil Palm fibers.

| Energy (MeV) | HVL Values | | | |
|---|---|---|---|---|
| | Untreated Jute Fiber | Treated Jute Fiber | Untreated Oil Palm Pressed Fruit Fiber | Treated Oil Palm Pressed Fruit Fiber |
| 0.1 | 2.120403496 | 1.217071734 | 1.533266071 | 1.61311625 |
| 0.15 | 2.639012467 | 2.026661401 | 2.238282706 | 2.352692015 |
| 0.2 | 2.965386276 | 2.618471759 | 2.685000983 | 2.821292698 |
| 0.3 | 3.493438873 | 3.438973809 | 3.310428317 | 3.478148545 |
| 0.4 | 3.969551362 | 4.054950643 | 3.818312377 | 4.012696536 |
| 0.5 | 4.416356678 | 4.589466865 | 4.266985278 | 4.490574908 |
| 0.6 | 4.839534586 | 5.065128475 | 4.69246814 | 4.938264711 |
| 0.8 | 5.578828941 | 5.89354839 | 5.434548301 | 5.712496466 |
| 1 | 6.296529746 | 6.671618278 | 6.13428796 | 6.453749159 |
| 2 | 9.290769919 | 9.87754559 | 9.028499781 | 9.513379114 |
| 3 | 11.69355524 | 12.3252284 | 11.30887123 | 11.90744367 |
| 4 | 13.8413511 | 14.35840032 | 13.14265514 | 13.92553891 |
| 5 | 15.42424766 | 15.7565966 | 14.50238267 | 15.33477535 |
| 6 | 16.76998738 | 16.84489006 | 15.6436828 | 16.55049589 |
| 8 | 19.06660011 | 18.85847423 | 17.45555522 | 18.62960835 |
| 10 | 21.19456888 | 20.38939237 | 19.06472794 | 20.21691912 |
| 12 | 23.28388145 | 21.90201107 | 20.20042789 | 21.82230032 |
| 14 | 24.93478691 | 23.20042992 | 21.57042885 | 23.09682213 |
| 16 | 27.12904816 | 24.82012562 | 23.16302204 | 24.93178237 |
| 18 | 28.24261409 | 25.74407726 | 23.65003943 | 25.69567216 |

| | | | | |
|---|---|---|---|---|
| 20 | 29.85901527 | 26.85326357 | 24.63545774 | 26.8888377 |

*Source: created by the authors.*

Table 5 - HVL Values (cm) for Bee-wax sample materials

| Energy (MeV) | HVL Values | | |
|---|---|---|---|
| | BM1 | BM2 | BM3 |
| 0.1 | 3.212048326 | 3.296932936 | 2.852704063 |
| 0.15 | 3.579418226 | 3.674444341 | 3.173053452 |
| 0.2 | 3.901230234 | 4.006816388 | 3.453854643 |
| 0.3 | 4.533929752 | 4.655243798 | 4.008067519 |
| 0.4 | 5.143949392 | 5.281845743 | 4.538204356 |
| 0.5 | 5.71780955 | 5.874925249 | 5.044078509 |
| 0.6 | 6.25369621 | 6.435189956 | 5.511535035 |
| 0.8 | 7.239437476 | 7.435924955 | 6.378518074 |
| 1 | 8.176798166 | 8.415248404 | 7.210818931 |
| 2 | 12.27939308 | 12.66938609 | 10.80375293 |
| 3 | 16.22231746 | 16.67501878 | 14.15360198 |
| 4 | 20.1507989 | 20.74197969 | 17.49669149 |
| 5 | 23.64737684 | 24.47553604 | 20.35387612 |
| 6 | 26.5400766 | 27.5058405 | 23.04269075 |
| 8 | 34.48527749 | 35.65571916 | 29.2348745 |
| 10 | 41.77749801 | 44.07987259 | 34.90536162 |
| 12 | 50.70201014 | 52.74129387 | 41.96619082 |
| 14 | 60.71184905 | 63.78341988 | 49.05396068 |
| 16 | 78.58811571 | 82.70656507 | 61.34154415 |
| 18 | 88.41163017 | 92.33098633 | 68.6216395 |
| 20 | 103.5568143 | 108.7392038 | 80.67918856 |

*Source: created by the authors.*

Table 6 - TVL Values (cm) for Jute and Palm fibers

| Energy (MeV) | TVL Values | | | |
|---|---|---|---|---|
| | Untreated Jute Fiber | Treated Jute Fiber | Untreated Oil Palm Pressed Fruit Fiber | Treated Oil Palm Pressed Fruit Fiber |
| 0.1 | 7.043827947 | 4.043024785 | 5.093399638 | 5.358656192 |
| 0.15 | 8.766609658 | 6.732423448 | 7.435414207 | 7.815473703 |
| 0.2 | 9.850799984 | 8.698374901 | 8.9193802 | 9.372131478 |
| 0.3 | 11.60495274 | 11.42402371 | 10.99700483 | 11.55415937 |
| 0.4 | 13.18656419 | 13.47025447 | 12.68415916 | 13.32988936 |
| 0.5 | 14.67081932 | 15.24587892 | 14.17461828 | 14.91736695 |
| 0.6 | 16.07658591 | 16.82599259 | 15.58804175 | 16.40456028 |
| 0.8 | 18.53246859 | 19.57794398 | 18.05317868 | 18.9765025 |
| 1 | 20.91661906 | 22.1626362 | 20.37766352 | 21.43889065 |
| 2 | 30.86326962 | 32.8124962 | 29.99202708 | 31.60276135 |
| 3 | 38.84514969 | 40.94352249 | 37.56725707 | 39.55567168 |
| 4 | 45.9799731 | 47.69757341 | 43.65895535 | 46.25963894 |
| 5 | 51.23824163 | 52.34228093 | 48.17587243 | 50.94102106 |
| 6 | 55.70869224 | 55.95751355 | 51.96718939 | 54.97955727 |
| 8 | 63.33787459 | 62.64649537 | 57.98609929 | 61.88621938 |
| 10 | 70.40683381 | 67.73209535 | 63.33165536 | 67.15915162 |
| 12 | 77.34737996 | 72.7569059 | 67.10436895 | 72.49211252 |
| 14 | 82.83156919 | 77.07015997 | 71.65541362 | 76.72598234 |
| 16 | 90.12074728 | 82.45067261 | 76.94589368 | 82.82158832 |
| 18 | 93.81993322 | 85.51997353 | 78.56373042 | 85.35917528 |
| 20 | 99.18950172 | 89.20461069 | 81.83721919 | 89.32278541 |

*Source: created by the authors.*

Table 7 - TVL Values for Bee-wax sample materials

| Energy (MeV) | TVL Values (cm) | | |
|---|---|---|---|
| | BM1 | BM2 | BM3 |
| 0.1 | 10.67019358 | 10.95217415 | 9.476477774 |
| 0.15 | 11.89056997 | 12.20623989 | 10.54065541 |
| 0.2 | 12.95960632 | 13.31035593 | 11.47345677 |
| 0.3 | 15.06138863 | 15.46438516 | 13.3145121 |
| 0.4 | 17.08783 | 17.54591177 | 15.07558855 |
| 0.5 | 18.99415219 | 19.51607924 | 16.75606611 |
| 0.6 | 20.77432914 | 21.37723831 | 18.30892308 |
| 0.8 | 24.04889074 | 24.70160802 | 21.18897839 |
| 1 | 27.16273555 | 27.9548501 | 23.95382199 |
| 2 | 40.79126086 | 42.08678959 | 35.88929039 |
| 3 | 53.88937214 | 55.39321336 | 47.01724807 |
| 4 | 66.939505 | 68.90336508 | 58.12275104 |
| 5 | 78.55488551 | 81.3059708 | 67.61411293 |
| 6 | 88.1642261 | 91.37242433 | 76.5461618 |
| 8 | 114.5576122 | 118.4457352 | 97.11615097 |
| 10 | 138.7818444 | 146.4301672 | 115.9531014 |
| 12 | 168.4284319 | 175.2027859 | 139.4086683 |
| 14 | 201.680397 | 211.8839345 | 162.9537301 |
| 16 | 261.0640695 | 274.7452621 | 203.7721989 |
| 18 | 293.6970782 | 306.7168975 | 227.9561522 |
| 20 | 344.0082907 | 361.223816 | 268.0104631 |

*Source: created by the authors.*

Table 8 - The Mean free path for the Jute and Oil Palm fibers

| Energy (MeV) | Mean Free Path (cm) for the investigated samples | | | |
|---|---|---|---|---|
| | Untreated Jute Fiber | Treated Jute Fiber | Untreated Oil Palm Pressed Fruit Fiber | Treated Oil Palm Pressed Fruit Fiber |
| 0.1 | 3.059095609 | 1.755863354 | 2.212035357 | 2.327234815 |
| 0.15 | 3.807290199 | 2.923854353 | 3.229159361 | 3.394217103 |
| 0.2 | 4.278148075 | 3.777656221 | 3.873637603 | 4.070264984 |
| 0.3 | 5.039966938 | 4.961390459 | 4.775938516 | 5.017907658 |
| 0.4 | 5.726852064 | 5.850057184 | 5.50866033 | 5.789097393 |
| 0.5 | 6.371455878 | 6.621201086 | 6.1559585 | 6.478530151 |
| 0.6 | 6.981972547 | 7.307435732 | 6.769800516 | 7.12441001 |
| 0.8 | 8.048548847 | 8.502593036 | 7.840395884 | 8.241390323 |
| 1 | 9.083972239 | 9.625110605 | 8.849906819 | 9.310791906 |
| 2 | 13.40374769 | 14.25028604 | 13.02537186 | 13.72490487 |
| 3 | 16.87023416 | 17.78154588 | 16.31525244 | 17.17880994 |
| 4 | 19.9688486 | 20.71479293 | 18.96084339 | 20.09030593 |
| 5 | 22.2524856 | 22.73196378 | 20.92251556 | 22.12340435 |
| 6 | 24.19397764 | 24.30203935 | 22.56906359 | 23.87731834 |
| 8 | 27.50728943 | 27.20702725 | 25.18304295 | 26.87684358 |
| 10 | 30.57729941 | 29.41567526 | 27.50458845 | 29.16684896 |
| 12 | 33.59154031 | 31.59792275 | 29.14305715 | 31.48292445 |
| 14 | 35.97329343 | 33.4711452 | 31.11955073 | 33.32167075 |
| 16 | 39.13894325 | 35.80787215 | 33.41717703 | 35.96895879 |
| 18 | 40.74547929 | 37.1408526 | 34.1197946 | 37.0710188 |
| 20 | 43.07745326 | 38.74107018 | 35.54145271 | 38.79239281 |

*Source: created by the authors.*

Table 9 - The Mean free path for the Bee-wax sample materials

| Energy (MeV) | Mean free path (cm) for the investigated samples | | |
|---|---|---|---|
| | BM1 | BM2 | BM3 |
| 0.1 | 4.634006191 | 4.756468798 | 4.115582005 |
| 0.15 | 5.164008923 | 5.301102629 | 4.57774848 |
| 0.2 | 5.628285512 | 5.780614132 | 4.982858965 |
| 0.3 | 6.54107797 | 6.716097142 | 5.782419133 |
| 0.4 | 7.421150278 | 7.62009266 | 6.547244919 |
| 0.5 | 8.249055483 | 8.475725522 | 7.277067051 |
| 0.6 | 9.02217651 | 9.284016637 | 7.951464262 |
| 0.8 | 10.44430055 | 10.72777206 | 9.202256393 |
| 1 | 11.79662616 | 12.14063714 | 10.40301271 |
| 2 | 17.7154195 | 18.27806048 | 15.58652078 |
| 3 | 23.40385696 | 24.0569669 | 20.41933139 |
| 4 | 29.07145764 | 29.92435124 | 25.24239005 |
| 5 | 34.1159533 | 35.31073446 | 29.36443614 |
| 6 | 38.2892369 | 39.68253968 | 33.24357568 |
| 8 | 49.75173882 | 51.44032922 | 42.17700847 |
| 10 | 60.27218921 | 63.59381359 | 50.35779211 |
| 12 | 73.14753859 | 76.08960312 | 60.54441538 |
| 14 | 87.58868354 | 92.02002356 | 70.76990581 |
| 16 | 113.3786848 | 119.3203513 | 88.49714154 |
| 18 | 127.5510204 | 133.2054561 | 99.000099 |
| 20 | 149.4009024 | 156.87751 | 116.3954652 |

*Source: created by the authors.*